DESIGN AND SIMULATION OF SOLAR PHOTOVOLTAIC BASED PROTON EXCHANGE MEMBRANE ELECTROLYZER FOR HYDROGEN PRODUCTION

Bala Murali Pydi
Associate Professor
Department of EEE
Aditya Institute of Technology and Management Tekkali
Srikakulam, India

Jaganmohan Rao Tarra
Assistant Professor
Department of EEE
Aditya Institute of Technology and Management Tekkali
Srikakulam, India

Patro Ganesh
Department of EEE
Aditya Institute of Technology And Management Tekkali
Srikakulam, India

Kethu Mukunda
Department of EEE
Aditya Institute of Technology and Management Tekkali
Srikakulam, India

Deepak Dehuri
Department of EEE
Aditya Institute of Technology and Management Tekkali
Srikakulam, India

Boori Sridhar
Department of EEE
Aditya Institute of Technology and Management Tekkali
Srikakulam, India

Corresponding Author: Bala Murali Pydi

Abstract:
In this paper, the proposed architecture of the Proton Exchange Membrane (PEM) electrolyzer system for green hydrogen production, solar photovoltaic, and the integration of the Maximum Power Point Tracking (MPPT) and the sun tracking systems, has been explained. The proposed architecture has been implemented on the MATLAB/Simulink platform, and the simulation results have been presented to validate the effectiveness of the proposed architecture for hydrogen production. The proposed architecture has been able to increase the gathered power significantly upon the integration of the sun tracking and the MPPT systems, even under varying temperature and irradiance conditions.

Keywords:
Solar PV, PEM electrolyzer, hydrogen production, MPPT, sun tracking, MATLAB/Simulink.

Introduction:

According to recent data released by prominent energy-related organizations, the world is currently producing hydrogen at a rate faster than ever before. The assistant editor of the journal, Shuo Sun, was responsible for the evaluation of the paper and granted the green light for publication. According to the Global Hydrogen Review 2023, the installed capacity of the electrolyzer has increased by more than four times between 2022 and 2023[1], [1], which may reach 560 GW by the year 2050 in net zero conditions. In addition, the 2023 report by IRENA also points out the need for a rapid increase in the manufacturing of electrolyzers in order to meet the growing demand, with notable cost reductions and a global drive for deployment. These new views offer a framework for judging the current scale of PV-based hydrogen systems and emphasize the importance of decentralized solar power coupled with efficient electrolyzers. The world's energy demand, in part, is met by renewable as well as non-renewable energy sources. According to the International Energy Agency (IEA) report, up to 85% of the world's energy supply in 2019 was met by fossil fuels, with the remaining 15% coming from different renewable sources[1]. This is in spite of the fact that the use of renewable energy sources has grown at a tremendous rate in recent years. The efficient use of solar energy for the production of fuels and chemicals can be considered a viable option in place of the unsustainable use of fossil fuels. The photoelectrochemical process of hydrogen production is one of the possibilities in this regard[2]. The solar fuel technologies are currently limited to small-scale designs with less than 100 W of output power, and these include thermochemical redox cycles, integrated photovoltaic(PV) and electrolyzer systems, photoelectrochemical cells (PECs) and photo-particulate systems. The recent advances in the integration of renewable energy and water electrolysis for hydrogen production have led to the discussion of smart cities, smart homes, and electric vehicles in the context of the essentiality of these organizations in the context of the supply of auxiliary services and optimization of microgrid energy management. For example, researchers have analysed two-stage stochastic-based scheduling for scheduling multi-energy microgrids with EVCSs, considering transaction costs in pool markets and bilateral contracts. The refuelling station can store up to 20 HFCs, each having a tank of 5 kg hydrogen. This will require the same amount of hydrogen to be refuelled. Using solar power to produce hydrogen provides promise for developing a more environmentally friendly and sustainable means of recharging electric cars, which could be a smart choice from both economic and environmental perspectives. Green hydrogen, or hydrogen derived from renewable energy sources, is emerging as a viable and competitive option to conventional hydrogen fuel cells, which are not contributing to the greenhouse effect and the problem of global warming. Figure 1 shows one of the largest green hydrogen installations in the world. Pilot-scale on-sun demonstrations are critical in investigating the viability of the scale-up of solar fuel technologies for their eventual use and application. However, there are several challenges in the scale-up of PEC devices or PV-EC devices depending on the specific device configuration and the experimental conditions and materials used. The direct and indirect methods are the two major routes for coupling PV systems with water electrolyzers to produce hydrogen fuel[3]. In the direct connection method, there is no need for the use of devices like direct current to direct current converters and maximum power point tracking devices. This minimizes energy transmission losses but requires the precise alignment of the solar array with the electrolyzer. In these kinds of issues, efficiency, sustainability, low cost, and long-term stability are sometimes at odds with each other. For example, devices developed by using semiconductors or noble metal catalysts are costly, but these are efficient, whereas photo particulate systems have low efficiency and selectivity but can be used in inexpensive polyethylene tubes or bags. Studies on renewable energy technologies have increased due to the increased need for sustainable and clean energy on a global level. Solar photovoltaic systems are one of the important technologies used to harness solar energy for generating electricity. There are several barriers to the rapid deployment of solar energy due to its intermittency and variability.

As such, effective methods of storing and converting energy are essential in order to improve the reliability and efficiency of solar energy systems. As an effective medium of energy that is able to solve the problems of storing energy in solar energy sources, hydrogen has been of significant interest. The production of green hydrogen, in particular, is achieved by passing an electric current through water in order to obtain hydrogen gas. This is an environmentally friendly type of fuel that is able to be used in various industries such as power generation, transportation, and industry. The use of solar photovoltaic systems in water electrolysis is an environmentally friendly way of converting solar energy into hydrogen gas in order to store it for later use[3].

In producing green hydrogen, various recent studies have focused on the integration of PV systems and water electrolysis, including technical, economic, and control-related perspectives. The results obtained from various studies in the recent literature and this review are compared in this section. Acosta et al. proposed an improved PV-alkaline freestanding hydrogen system using a 10 kW PV array to achieve a production rate of 0.9 Nm3/h and an LCOH of 6.7 USD/kg H2. However, due to better load management and dynamics, better production rates were achieved in the systems proposed in this study, especially those using PEM systems and MPPT control.

SIMULATION DIAGRAM

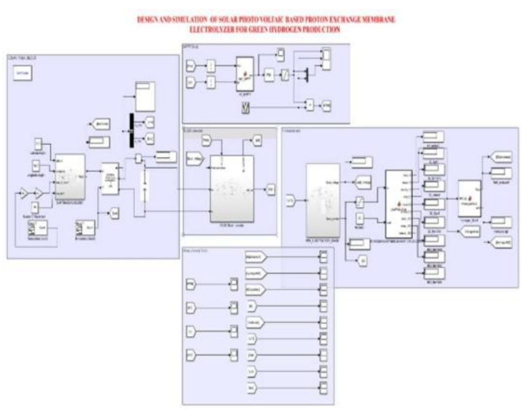

SOLAR PV ARRAY

A solar photovoltaic (PV) array is a configuration of solar panels connected to generate electricity from sunlight. It is the main source of power in a solar power system. When several solar panels are connected in series and parallel, a solar PV array is produced. Numerous sun cells make up each solar panel. The array increases its power output to meet the required electrical load. A solar PV array's operation is based on the photovoltaic effect. When sunlight strikes solar cells, the semiconductor material—typically silicon—absorbs photons and releases electrons. As these electrons move across the external circuit, electric current is produced. Direct current (DC) electricity is converted into alternating current (AC) for usage in homes and businesses using an inverter.

A solar PV array is made up of a number of essential parts. These include solar cells, solar modules (panels), cables, connectors, junction boxes, DC combiner boxes, and mounting structures. A mounting mechanism holds the panels at a preset tilt angle to optimize sunlight[4].

The combiner box collects power from multiple strings while guarding against over currents and lightning surges. A solar PV array's panels can be connected in series or parallel. A series connection raises the output voltage, while a parallel connection raises the output current. GPS and astronomical techniques are used by the advanced array tracking systems[5].

Sun Tracking Mechanism

The term given to such a system is sun tracking. This is an advantage over fixed solar panel systems because of increased solar power absorption. In this project, a dual-axis sun tracking system is used[6]. Instead of using conventional light sensor devices to track the sun's movement, solar panel orientation is achieved by using solar panel parameters.

The solar panel tracking is achieved by using solar elevation angle and solar azimuth angle parameters[7]. These parameters define the sun's position in the sky. Using these parameters, it is possible to find the required panel tilt angle and panel azimuth angle in order to maintain the solar panel in such an orientation that it is almost perpendicular to solar radiation.

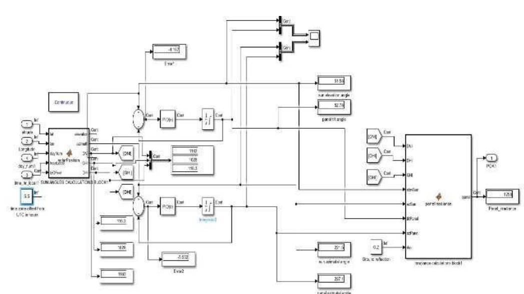

The sun tracking system uses two axes: an azimuth axis for horizontal movement and an elevation axis for vertical movement. The movement of these axes is achieved by using actuators whose movements are controlled by a PID controller in MATLAB/Simulink[6]. The PID controller compares the required values (reference values obtained by calculating solar panel parameters) with the current values by minimizing the error by adjusting control signals supplied to the actuators. Unlike other tracking systems, this technique uses time and location-based solar position algorithms[7], which are accurate and work well in different environmental conditions. The PID control system also helps in maintaining stability and reducing error, thereby ensuring smooth tracking of the sun in different seasons of the year**.**

DC-DC Converter

A power electronic circuit called a DC-DC boost converter or step-up converter is used to transfer power efficiently from a smaller DC input voltage to a higher DC output voltage[8]. This converter is often used in electronic circuits when the voltage supplied by the power source, like a battery, solar cell, or fuel cell, is insufficient to meet the requirements of the load. The boost converter is compact, lightweight, and suited for modern electronic devices due to its capability to boost voltage without using transformers by employing high-frequency switching components[9].

The basic components of a boost converter include an inductor, a switch usually in the form of a controlled switch such as a MOSFET, a diode or synchronous switch, an output capacitor, and a control circuit. These components of the boost converter store the supplied electrical energy and discharge it in the form of an increased voltage level. However, in order to maintain the stability of the output voltage in accordance with varying input voltages or other situations, the control circuit is used to control the switching action.

The two states of switching of a boost converter can be considered in order to understand the working of such a boost converter. In this case, when the switch is turned on, the input voltage is connected in series with the inductor[8]. This increases the inductor current, thus storing energy in the inductor in the form of a magnetic field. At this time of operation of the boost converter, referred to as the energy storage phase, the diode reverse biases the output of the boost converter, and the stored energy in the capacitor is supplied to the load.

When the switch is closed, the inductor maintains the flow of the current, thereby inverting the polarity of the voltage, which then transfers the energy from the inductor to the capacitor by increasing the voltage level, thereby forward biasing the diode. The voltage level was therefore increased above the original voltage level. By repeating the above process at a high frequency, the voltage level can be increased continuously by this converter[10].

MPPT Controller

In order to maximize the amount of power produced by the solar panels, the solar power system utilizes an MPPT controller[10], which is an advanced form of charge controller. The MPPT controller is known as Maximum Power Point Tracking. The voltage and the current produced by the solar panels are not fixed due to the temperature and the amount of sunlight. The MPPT controller will always track the maximum power point of the solar panel and adjust the operating points to maximize the power extraction. The I-V and the P-V characteristics of the solar panel are the basis for the operation of the MPPT controller. The solar panel has the capability to produce the maximum power at the specific voltage and the current points. We call the position Maximum Power position, or MPP[11]. In order to find this, the MPPT controller uses algorithms like the Hill Climbing, Incremental Conductance, and Perturb and Observe method. The majority of the MPPT controller comprises a microcontroller, sensors, control circuits, and a DC-DC converter. The buck, boost, or buck-boost type of the DC-DC converter changes the voltage and current of the solar panel according to the requirements of the battery or load. The microprocessor of the MPPT controller calculates the power, voltage, and current of the panel and regulates the switching of the converter to run at the MPP[12].

MPPT Techniques

Solar photovoltaic systems incorporate maximum power point tracking control strategies to ensure that the maximum power that can be produced by the solar panel is harnessed. The voltage and current produced by the solar panel vary according to the intensity of the sun, temperature, and shade. The efficiency of the solar power system is improved by using maximum power point tracking strategies to adjust the operating point of the solar panel to ensure that it always operates at its maximum power point[13].

Incremental Conductance (INC) MPPT Technique

The Incremental Conductance (INC) approach is one advanced method used in Maximum Power Point Tracking (MPPT) for solar photovoltaic (PV) systems. It is designed to accurately track the maximum power point of a solar panel by analysing the relationship between voltage and current. Compared to simpler methods like Perturb and Observe (P&O), the INC technique provides faster and more precise tracking, especially in scenarios with rapidly changing environmental conditions[14]. PEM electrolyzer cells by adding the three overpotentials and the reversible voltage. The Incremental Conductance approach is based on the slope of a solar panel's power-voltage (P-V) curve. Power (P) is the result of multiplying voltage (V) by current (I). There is no change in power in relation to voltage since the P-V curve's slope is zero at the highest power point. The mathematical expression for this condition is dP/dV = 0. By raising this, the controller applies the condition dI/dV = –I/V at the maximum power point. The INC algorithm continuously calculates the incremental conductance (current divided by voltage) and compares it to the instantaneous conductance (current divided by voltage).The INC approach uses a microcontroller in conjunction with voltage and current sensors in practical applications[15].

PEM electrolyzer simulation design

In this study, we propose a simulating approach that provides a safety-oriented alternative to actual electrolyzers, eliminating the need for supplementary components such as water supply, cooling systems, hydrogen tanks, etc., making it a cost-effective and reliable option for smart grid testing. The emulator design can accurately replicate characteristics(V–I) the and electrical dynamic behaviour of PEM electrolyzers under various conditions. This proposed emulator is designed for use with different types of water electrolyzers and DC electronic loads, with equipment**.**[16].

$$V_{elc} = N_{cell} \cdot (E_{rev} + V_{ohm} + V_{act} + V_{con}) \qquad (1)$$

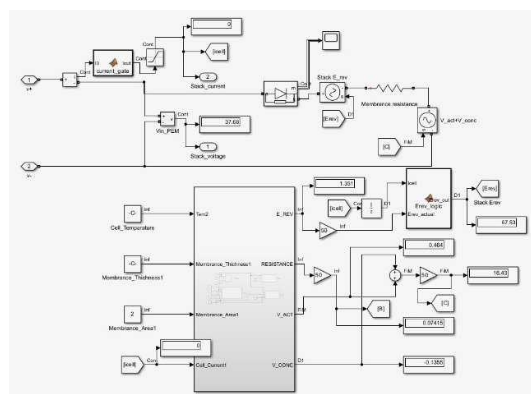

Reversible Voltage

According to the Nernst definition, reversible voltage (Erev) is the lowest electrical potential necessary to influence the dissociation of water into hydrogen and oxygen. Assuming that the applied liquid water equals the sutured vapor pressure [17]

$$E_{rev} = E^0_{rev}(\frac{RT}{2F}) \ln (\frac{p_{H2}p^{\frac{1}{2}}_{O2}}{p^{sat}_{H20}}) \quad (2)$$

Equation (6) describes the reversible voltage at standard pressure (P_{std}= 1 atm) as the term, which is highly dependent on temperature. The partial pressures of hydrogen, oxygen, and saturated water vapor are denoted by the

P_{H2} , P_{O2} $and P^{sat}_{H20}$ values, respectively. Equations (4) and (5) of Dalton's law, the August–Roche–Magnus formula (6) of partial pressures, and three assumptions can be used to obtain these values.

Only water and oxygen vapor are present at the anode, only water and hydrogen vapor are present at the cathode, hydrogen and oxygen act like ideal gases, and their solubility in water is thought to be minimal.

where pan and P_{cat} are the pressure at the cathode P_{ca} and the anode pan were measured from the gas separator.

Only water and oxygen vapor are present at the anode, only water and hydrogen vapor are present at the cathode, hydrogen and oxygen act like ideal gases, and it is thought that their solubility in water is minimal.

$$E^0_{rev} = 1.229 - 8.5 \times 10^{-4}(T - 298.15) \quad (3)$$

$$P_{H2} = P_{cat} - P^{sat}_{H20} \quad (4)$$

$$P_{O2} = P_{an} - P^{sat}_{H20} \quad (5)$$

$$P^{sat}_{H20} = 6.1078 \times 10^{-3} \exp [17.694 \times (\frac{T-273.15}{T-34.85})]$$

(6)

where the gas separator was used to measure the pressure at the cathode (P_{ca})and anode (P_{an}).

Ohmic overpotential

Two factors are usually responsible for the ohmic overpotential: the resistance of electrons in the electrodes and other electronic conductors (R_{ele}) and the resistance of ions in the PEM electrolyzer membrane (R_{mem}). It is significant to observe that the membrane resistance is significantly higher than the electrical resistance.

$$R_{ohm} \approx R_{mem} = \frac{\delta_{mem}}{A_{mem}\sigma_{mem}} \quad (7)$$

Where the δ_{mem}, σ_{mem} , A_{mem} stand for the membrane's thickness, conductivity, and area, respectively. Both the cell's temperature and the membrane's water content (λ_{mem}) have an impact on the membrane's conductivity.

$$\sigma_{mem} = 5.14 \times 10^{-3}\lambda_{mem} - 3.26 \times 10^{-3}\exp [1268(\frac{1}{303} - \frac{1}{T})] \quad (8)$$

A PEM electrolyzer contains more water at both the anode and the cathode than a PEM fuel cell. Because the membrane's water content usually ranges from 14 to 22, researchers have often concluded that it is fully hydrated. We use water content parameters of 22 in this investigation[18].

Activation overpotential

The extra voltage needed to propel the electrolysis reaction above the reversible voltage in a PEM electrolyzer is known as the activation overpotential. The materials and active surface area of the catalyst, as well as temperature, all have an impact on the electrochemical reaction kinetics at the electrode's surface, which results in this overpotential. The activation overpotential is frequently described by the Butler-Volmer equation.

The rate of hydrogen reaction at the cathode is substantially faster than the rate of oxygen reaction at the anode. Consequently, a lot of research ignores the impact of overpotential activation at the cathode. By increasing the size of the active catalyst site, the roughness of the electrode can be adjusted to raise the activation overpotential.

$$V_{act} = \frac{RT}{\alpha_{an}F}\sinh^{-1}(\frac{i}{2i_{0,an}}) + \frac{RT}{\alpha_{cat}}\sinh^{-1}(\frac{i}{2i_{0,cat}})$$

(9)

The basic electrochemical parameters of exchange current density ($i_{an,cat}$) and charge transfer coefficient ($\alpha_{an,cat}$) must be taken into account in order to calculate the activation overpotential. These parameters are particularly important at the anode electrode, and any errors in their calculation can significantly affect the polarization curve and the PEM electrolyzer's overall performance.

The exchange current density and transfer charge coefficient are significantly affected by temperature changes. The exchange current density can be expressed using an empirical equation found in references.

$$i_{0,an} = i_{0,an}^{ref} exp\left[-\frac{E_{act,an}}{R}\left(\frac{1}{T}-\frac{1}{T_{ref}}\right)\right] \quad (10)$$

where $i_{0,an}^{ref}$ exchange current density at reference condition and is activation energy required to the electrons transport in the electrodes[18].

Concentration overpotential

When the current density in a PEM electrolyzer is high, concentration overpotential happens, which results in an accumulation of hydrogen and oxygen molecules that obstruct the active sites and slow down the reaction rate. Limiting the current is necessary to attain high efficiency. The efficiency of PEM electrolyzers is significantly impacted by concentration overpotential, sometimes referred to as mass transport overpotential. Researchers measure these concentration losses using equation (11) with the diffusion limit current density (i_{Lim}) parameter. The maximum current density at which diffusion can take place beyond which the synthesis of hydrogen and oxygen will cease is represented by the parameter[18].

$$V_{cons} = \frac{RT}{2a_{an}F} ln \left(\frac{i_{Lim}}{i_{lim-i}}\right) \quad (11)$$

Flow of gases products and water costumed

If hydrogen and oxygen products behave like ideal gases, equations that can be used to determine their mass flow rate can be derived based on Faraday's Law[18], [19].

$$Q_{H_2-m} = Q_{H_20-m} = N_{cell}\frac{I_{el}}{2F}\eta_F \quad (12)$$

$$Q_{0_2-m} = N_{cell}\frac{I_{el}}{4F}\eta_F \quad (13)$$

The variables in this equation are Q_{H_2-m} and Q_{0_2-m}, which stand for the mass flow rates of oxygen and hydrogen, respectively. The water electrolyzer's water consumption is indicated by Q_{H_2O} m. The PEM electrolyzer's cell count, current, and Faraday efficiency are denoted by the values N_{cell}, I_{el}, and 5_F, respectively[20] Equations (12) and (13) in combination with the ideal gas law can be used to determine the volume flow rate of hydrogen and oxygen in normal meter cubes per hour (Nm3/h).

$$Q_{H_2-V} = (5_F \times \frac{N_{cell}RT}{2F\rho_{H_2}} \times 3600)\, I_{el} \quad (14)$$

$$Q_{0_2-V} = (5_F \times \frac{N_{cell}RT}{4F\rho_{0_2}} \times 3600)\, I_{el} \quad (15)$$

where Q_{H_2-V} and Q_{0_2-V} represents the volume, flow rates of hydrogen and oxygen, respectively, while ρ_{H_2} and ρ_{0_2} denote the partial pressure of hydrogen and oxygen, respectively.

PEM electrolyzer electrical modelling validation

By replacing each term with its appropriate expression and the constant parameters with their numerical values, the following Equation (1) can be written as Equation (16) for the PEM electrolyzer cell. The PEM electrolyzer temperature, anodic pressure, and cathodic pressure are among the inputs required to compute the polarization curve (V–I characteristic). For simplicity, it is assumed that the charge transfer coefficient, αan, only minimally changes with temperature, but the thickness of the membrane, δ_{mem}, still relies on the membrane shape. However, a number of variables, including catalyst materials, electrode roughness, electrode porosity, and the concentration and size of the catalyst particles, affect other parameters, such as the exchange current density at reference condition $i_{0,an}^{ref}$ activation energy $E_{act,an}$ and limit current density i_{lim}. Therefore, identifying them using the proper identification techniques is the best way to get these parameters. In this study, we suggest estimating these parameters using Particle Swarm Optimization (PSO). In order to validate the accuracy of the developed PEM electrolyzer model, a comprehensive analysis of the experimental data of previously tested PEM electrolyzers is conducted based on relevant literature. The polarization curve of the PEM electrolyzer is successfully reproduced by implementing the developed model and estimating the required parameters by using the Incremental Conductance (INC) algorithm in MATLAB.[18].

$$V_{cell} = 1.229 - 8.5\times10^{-4}(T-298.15) + 4.3087\times10^{-5}T \times \ln\left(\frac{(P_{cat}-6.1078\times10^{-3}\exp[17.694\times\frac{T-273.15}{T-34.85}])\times(P_{an}-6.1078\times10^{-3}\exp[17.694\times\frac{T-273.15}{T-34.85}])}{6.10786.1078\times10^{-3}\exp[17.694\times\frac{T-273.15}{T-34.85}]}\right) +$$
$$\frac{\delta_{mem}}{A_{mem}\times0.1113-.26\times10^{-3}\exp[1268(\frac{1}{303}-\frac{1}{T})]} +$$
$$8.6174\frac{10^{-5}T}{\alpha_{an}}\sinh^{-1}\left(\frac{i}{2i_{0,an}^{ref}\exp[\frac{-E_{act,an}}{R}(\frac{1}{T}-\frac{1}{T_{ref}})]}\right) +$$
$$\frac{4.3087\times10^{-5}T}{\alpha_{an}}\ln\left(1+\frac{i}{i_{lim}}\right) \quad (16)$$

In order to validate the accuracy of the developed PEM electrolyzer model, the experimental data from previously tested electrolyzers reported in the literature was analysed. The required parameters were estimated using the Incremental Conductance algorithm, referred to as the I&C algorithm, implemented in MATLAB. The estimated parameters were used to successfully reproduce the polarization curve for the PEM electrolyzer.

As the polarization curve is more sensitive to temperature than pressure, the study is performed only on the temperature effects while the pressures are kept constant at: ($P_{an} = 1$ bar and $P_{cat} = 31$ bar). In the experiment, the polarization curves were plotted for four different temperatures: 318.15 K, 323.15 K, 328.15 K, and 333.15 K, within the range of 0 to 2 A/cm². The experimental cell voltage data, referred to as $V_{cell-exp}$ and the unknown parameter vector φ is given by:

$$\varphi = [\delta_{mem}, \alpha_{an}, i_0^{ref}, E_{act,an}, i_{lim}]^T \quad (17)$$

In order to use the Incremental Conductance algorithm appropriately, a cost function is formulated that assesses the deviation of the predicted and experimentally measured voltages of the cells. The cost function is a measure of the accuracy of the proposed model by calculating the total squared errors of the expected and experimental voltage levels. The cost function is written as:

$$\text{Cost Function} = \sum_{j=1}^{K}(V_{cell-exp} - V_{cell})^2 \quad (18)$$

where:

$V_{cell-exp}$ (j): Represents the experimental cell voltage for the jth data point.

V_{cell} (j): Is the predicted cell voltage based on the model for the jth data point.

K: Total number of data points being considered[16].

Results

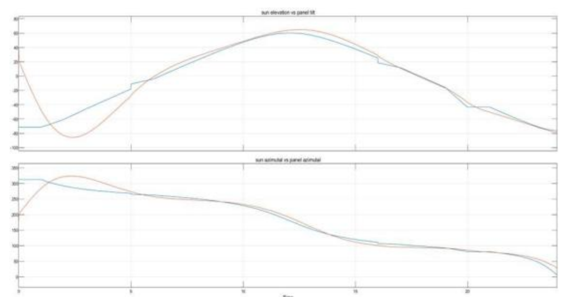

a-sun vs panel angles tracking

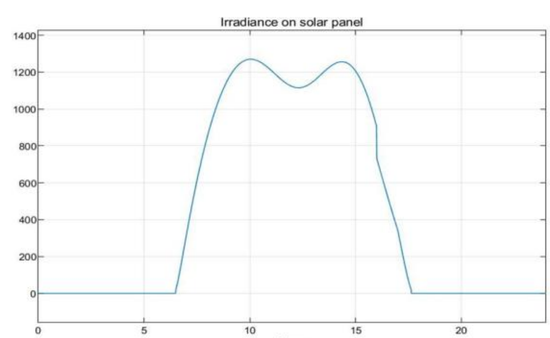

b-Irradiance on solar panel

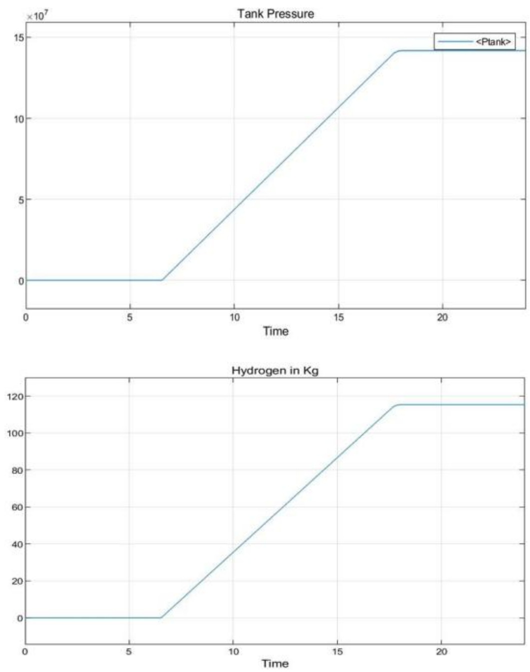

c-Results with boost converter

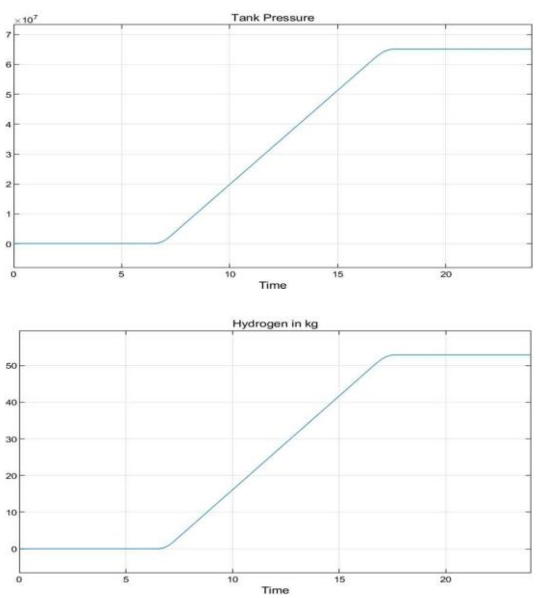

d-Results without boost converter

Comparative Analysis

The performance evaluation of the solar-powered hydrogen production system was done under changing conditions of irradiance and temperature, with and without the boost converter. The absence of the boost converter causes the PV array to operate away from the MPP, and hence the power transfer is less to the electrolyzer. The consequence is that the electrolyzer is not getting enough voltage and current, and hence the rate of production of hydrogen is less.

Parameter	With Boost Converter	Without Boost Converter
PV Voltage	Stable and well regulated	Highly fluctuating
Stack Current	Smooth and controlled	Oscillatory and unstable
H_2 Production Rate	High and nearly constant	Low and inconsistent
Hydrogen Mass	115 kg	53 kg
Tank Pressure	Higher and steady	Lower with slow rise
System Efficiency	High	Reduced
Electrolyzer Stress	Low	High

On the other hand, the inclusion of the boost converter helps to track the MPP, and hence the PV array is operating close to the MPP even under changing environmental conditions. The consequence is that the electrolyzer is getting enough voltage and current, and hence the rate of production of hydrogen is high. The results clearly indicate the efficiency of the system with the boost converter compared to the system without the boost converter.

Conclusion

In this article, a solar PV-based PEM electrolyzer system for hydrogen production employing sun tracking and MPPT was designed and simulated. The findings verify that combining dual-axis sun monitoring with MPPT optimizes solar energy use and boosts hydrogen production. The suggested technology offers a workable way to produce green hydrogen in an efficient and ecological manner.

Future Scope

Future research in PEM electrolyzer systems and renewable hydrogen production can greatly improve the suggested framework's practical application, economic feasibility, and technological robustness. Although the modelling and simulation used in this work offer insightful information, a number of significant research extensions might be undertaken to improve the overall contribution and close the gap between theoretical analysis and practical application.

Validating the established models and simulation findings experimentally is a crucial avenue for future research. To confirm system correctness and dependability, real-world research in controlled laboratory or pilot-scale settings is required, even if simulation-based studies are crucial for initial design and performance evaluation. Real-time performance of the PEM electrolyzer under fluctuating power inputs, dynamic responsiveness under changing temperature and irradiance conditions, and a thorough assessment of system efficiency would all be possible with experimental validation. Additionally, it would assist in identifying real-world difficulties that simulations might not adequately represent, such as problems with temperature management, voltage instability, and control constraints. The suggested system's legitimacy and industry usefulness will be greatly enhanced by the inclusion of real-world testing.

References

[1] M. Yessef, Y. Hakam, M. Tabaa, S. M. Irshad, and Z. M. S. El-Barbary, "Integration of Photovoltaic Systems With Hydrogen Production: A Review of Current Technologies and Future Perspective," *IEEE Access*, vol. 13, pp. 136716–136730, 2025, doi: 10.1109/ACCESS.2025.3595057.

[2] H. C. Lee, J. H. Park, S.-I. In, and J. Yang, "Recent advances in photoelectrochemical hydrogen production using I–III–VI quantum dots," *Nanoscale*, vol. 16, no. 19, pp. 9295–9310, 2024, doi: 10.1039/D4NR01040J.

[3] X. Cao *et al.*, "Hydrogen Production System Using Alkaline Water Electrolysis Adapting to Fast Fluctuating Photovoltaic Power," *Energies*, vol. 16, no. 8, p. 3308, Apr. 2023, doi: 10.3390/en16083308.

[4] H. L. Walpita *et al.*, "Operation and Maintenance of Floating PV Systems: A Review," *IEEE J. Photovolt.*, vol. 15, no. 3, pp. 400–415, May 2025, doi: 10.1109/JPHOTOV.2025.3548322.

[5] Yinghua Dong, Hongtao Li, Junjun Zhang, Fubao Wu, and Mingchang Ding, "Model of long-term yield evaluation for PV station," in *8th Renewable Power Generation Conference (RPG 2019)*, Shanghai, China: Institution of Engineering and Technology, 2019, p. 9 (5 pp.)-9 (5 pp.). doi: 10.1049/cp.2019.0266.

[6] H. A. Issa, L. M. Abdali, H. Alhusseini, and V. I. Velkin, "Design, modeling, and control of a dual-axis solar tracker using fractional order PID controllers for enhanced energy efficiency," *Results Eng.*, vol. 27, p. 106073, Sep. 2025, doi: 10.1016/j.rineng.2025.106073.

[7] M. H. M. Sidek, N. Azis, W. Z. W. Hasan, M. Z. A. Ab Kadir, S. Shafie, and M. A. M. Radzi, "Automated positioning dual-axis solar tracking system with precision elevation and azimuth angle control," *Energy*, vol. 124, pp. 160–170, Apr. 2017, doi: 10.1016/j.energy.2017.02.001.

[8] J. N. Rai, N. Gupta, and P. Bansal, "Design and Analysis of DC-DC Boost Converter," *Int. J. Adv. Res. Innov.*, vol. 4, no. 3, pp. 34–37, 2016, doi: 10.51976/ijari.431607.

[9] S. Kumar and A. Usmam, "Effective Design Analysis of a DC-DC Boost Converter with Experimental Validation," in *2018 Internat2018 International Conference on Computation of Power, Energy, Information and Communication (ICCPEIC)ional conference on computation of power, energy, Information and Communication (ICCPEIC)*, Chennai, India: IEEE, Mar. 2018, pp. 261–268. doi: 10.1109/ICCPEIC.2018.8525165.

[10] H. I. Cristian and N. Bizon, "Performance of the Global MPPT Algorithms — A brief overview and case studies," in *2016 8th International Conference on Electronics, Computers and Artificial Intelligence (ECAI)*, Ploiesti, Romania: IEEE, Jun. 2016, pp. 1–8. doi: 10.1109/ECAI.2016.7861125.

[11] J. W. Zanotti and D. C. Martins, “Input characteristic impedance technique of power converters circuits applied to the maximum power point tracker of photovoltaic panels,” in *2014 IEEE Asia Pacific Conference on Circuits and Systems (APCCAS)*, Ishigaki, Japan: IEEE, Nov. 2014, pp. 292–295. doi: 10.1109/APCCAS.2014.7032777.

[12] S. Abssane, A. Outzourhit, and F. Z. Amatoul, “Comparison between incremental conductance and perturb and observe algorithms in photovoltaic system under low temperature and irradiation levels,” *Int. J. Electr. Comput. Eng. IJECE*, vol. 14, no. 5, p. 4897, Oct. 2024, doi: 10.11591/ijece.v14i5.pp4897-4906.

[13] J. A. Carrasco, F. G. De Quiros, H. Alaves, and M. Navalon, “An Analog Maximum Power Point Tracker With Pulsewidth Modulator Multiplication for a Solar Array Regulator,” *IEEE Trans. Power Electron.*, vol. 34, no. 9, pp. 8808–8815, Sep. 2019, doi: 10.1109/TPEL.2018.2886887.

[14] Associate Professor, Department of EEE, Mahatma Gandhi Institute of Technology, India, Dr. P. C. Sekhar, Mr. K. B.Kumar,and Researchscholar, S. V. National Institute of Technology, Surat, India, “INCREMENTAL CONDUCTANCE MPPT TECHNIQUE WITH BOOST CONVERTER,” *Eng. Technol. J.*, vol. 08, no. 06, Jun. 2023, doi: 10.47191/etj/v8i6.04.

[15] P. Ganesan, G. S, and A. J. G. A, “Modelling and Simulation of Incremental Conductance Algorithm for Solar Maximum Power Point Tracker,” in *2022 IEEE Delhi Section Conference (DELCON)*, New Delhi, India: IEEE, Feb. 2022, pp. 1–6. doi: 10.1109/DELCON54057.2022.9753007.

[16] A. S. Tijani, F. H. Shukri, A. H. Abdol Rahim, S. Hanapi, and K. I. Sainan, “Mathematical modelling and simulation analysis of PEM electrolyzer system for hydrogen production,” in *3rd IET International Conference on Clean Energy and Technology (CEAT) 2014*, Kuching, Malaysia: Institution of Engineering and Technology, 2014, p. 19 (7 .)-19 (7 .). doi: 10.1049/cp.2014.1466.

[17] J. Delmas *et al.*, “Improved hydrogen storage capacity through hydrolysis of solid NaBH4 catalyzed with cobalt boride,” *Int. J. Hydrog. Energy*, vol. 36, no. 3, pp. 2145–2153, Feb. 2011, doi: 10.1016/j.ijhydene.2010.11.036.

[18] M. Koundi *et al.*, “Electrical modelling, design, and implementation of a hardware PEM electrolyzer emulator for smart grid testing,” *Int. J. Emerg. Electr. Power Syst.*, vol. 26, no. 1, pp. 85–105, Feb. 2025, doi: 10.1515/ijeeps-2023-0213.

[19] J. Delmas *et al.*, “Improved hydrogen storage capacity through hydrolysis of solid NaBH4 catalyzed with cobalt boride,” *Int. J. Hydrog. Energy*, vol. 36, no. 3, pp. 2145–2153, Feb. 2011, doi: 10.1016/j.ijhydene.2010.11.036.

[20] J. Delmas *et al.*, “Improved hydrogen storage capacity through hydrolysis of solid NaBH4 catalyzed with cobalt boride,” *Int. J. Hydrog. Energy*, vol. 36, no. 3, pp. 2145–2153, Feb. 2011, doi: 10.1016/j.ijhydene.2010.11.036.